

## TAPER ANGLE OPTIMIZATION OF SCARF REPAIRS IN CARBON-EPOXY LAMINATES

R.D.S.G. Campilho<sup>1,2</sup>, A.M.G. Pinto<sup>3</sup>, M.F.S.F. de Moura<sup>2</sup>, I.R. Mendes<sup>3</sup>,  
M.D. Banea<sup>2</sup>, L.F.M. da Silva<sup>2</sup>

<sup>1</sup>Instituto de Engenharia Mecânica e Gestão Industrial,  
Campus da FEUP, Rua Dr. Roberto Frias, nº 400, 4200-465 Porto, Portugal.  
E-mail: raulcampilho@hotmail.com

<sup>2</sup>Departamento de Engenharia Mecânica, Faculdade de Engenharia da Universidade do Porto,  
Rua Dr. Roberto Frias, 4200-465 Porto, Portugal.

<sup>3</sup>Instituto Superior de Engenharia do Porto  
Rua Dr. António Bernardino de Almeida, 431, 4200-072 Porto, Portugal.

### ABSTRACT

The increasing use of Carbon-Fibre Reinforced Plastic (CFRP) laminates in high responsibility applications introduces an issue regarding their handling after damage. The availability of efficient repair methods is essential to restore the strength of the structure. The availability of accurate predictive tools for the repairs behaviour is also essential for the reduction of costs and time associated to extensive tests. This work reports on a numerical study of the tensile behaviour of three-dimensional (3D) adhesively-bonded scarf repairs in CFRP structures, using a ductile adhesive. The Finite Element (FE) analysis was performed in ABAQUS<sup>®</sup> and Cohesive Zone Models (CZM's) was used for the simulation of damage in the adhesive layer. A parametric study was performed on two geometric parameters. The use of over-laminating plies covering the repaired region at the outer or both repair surfaces was also tested as an attempt to increase the repairs efficiency. The results allowed the proposal of design principles for repairing CFRP structures.

**KEY WORDS:** Carbon-Epoxy; Cohesive Zone Models; Composite; Finite Element Analysis; Repair.

### 1. INTRODUCTION

CFRP components are being more and more used in structures demanding a high performance because of their superior characteristics (such as high strength, high stiffness, long fatigue life and low density). However, CFRP materials usually show a high sensitivity to temperature, moisture and impacts. Thus, repair strategies should always be considered over replacement [1]. Adhesively-bonded repairs are an option, but these typically do not restore the initial strength and stiffness of the components without a significant weight penalty. Thus, a substantial amount of research has been carried out recently on efficient repair techniques and adhesives technology [2]. Several studies are available for the repair of composite panels [3], including FE works describing predictive techniques for the repairs strength [2]. Unlike the single-strap solution, scarf repairs do not cause a substantial bending of the components, which reduces peel stresses [4]. Moreover, shear stress distributions along the bond length are practically uniform due to the tapering effect at the scarf edges [5]. The outcome of this optimization of stresses is a higher efficiency [6] and the substantial or full strength recovery typically achieved by this method usually makes scarf repairs as permanent [7]. Scarf repairs are also flush with the damaged structure, preventing aerodynamic disturbance. Despite all of these advantages, scarf repairs are more difficult to execute,

which reflects on higher costs. In addition, they require a large repair area, since relatively small angles are necessary to restore the strength of components [7, 8]. This repair is fabricated by machining a tapered cavity to remove the damaged material. A conical patch is then adhesively-bonded to the structure [5, 9].

In tension, experimental and FE studies show an exponentially increasing strength of scarf assemblies (joints or repairs) with the reduction of the scarf angle ( $\alpha$ ), due to the corresponding increase of bond area [7, 8]. On the failure modes, the literature reports that values below  $\alpha \approx 2^\circ$  lead to cross-sectional failures of the laminates outside the repaired region, while bigger values typically yield failures of the adhesive bond [5, 9]. Odi and Friend [10] compared the stress distributions between three FE approaches to simulate stepped and  $\alpha = 3^\circ$  CFRP scarf repairs under tension, using equivalent orthotropic elastic properties for the CFRP components. For the scarf repairs, shear stresses in the adhesive were nearly constant, leading to a high efficiency, as the adhesive failed simultaneously at the entire bond length. 3D ply-level analyses of composite repairs have recently become feasible, as a result of the advancement of desktop computers. In recent years, fairly accurate predictions were achieved on the static strength of adhesively-bonded repairs using CZM's coupled with FE simulations [11, 12]. This technique, which accounts

for the progressive damage evolution, is particularly meaningful for scarf repairs due to the difference between damage initiation and failure loads [13]. The work of Campilho et al. [5] validates with experiments a trapezoidal CZM applied to tensile loaded Two-Dimensional (2D) scarf repairs on CFRP laminates, for values of  $\alpha$  between  $2^\circ$  and  $45^\circ$ . To account for the experimental fractures, the cohesive failure of the adhesive layer and composite interlaminar and intralaminar (in the transverse and fibre directions) failures were considered. The corresponding cohesive laws were estimated by inverse modelling. The accurate predictions validated the proposed technique.

This study reports on the tensile behaviour of 3D scarf repairs in CFRP structures, using a ductile adhesive (Araldite® 2015). Since the proposed numerical methodology was already validated with experiments in previous works, giving accurate estimations [11, 12], this research is restricted to a purely numerical optimization of the repairs that will allow the definition of principles for repairing. Traditionally, the design of scarf repairs is based on 2D models, as a simplification of the 3D geometry [14]. The primary motivation for this work stems from the known inconsistencies between the 2D approximations and the 3D repair [3]. In fact, with the 2D simplification, stresses along the scarf bond are regarded as constant in the width direction of the repairs, thus neglecting the concentrations at the scarf edges near the longitudinal mid-plane of the 3D repair [7]. Moreover, the 2D simplified geometry does not capture the typical 3D stress effects of these repairs that may result on a premature catastrophic failure at or near the interfaces between the composite and the adhesive layer [15]. The FE analysis was performed in ABAQUS® and used CZM's for the simulation of damage in the adhesive layer. Trapezoidal cohesive laws in each pure mode were used to account for the ductility of the adhesive. A parametric study was performed on the repair width ( $b$ ) and  $\alpha$ . The use of over-laminating plies covering the repaired region at the outer or both repair surfaces was also tested to increase the repairs efficiency. The results obtained allowed the establishment of design principles for repairing.

## 2. NUMERICAL ANALYSIS

The cohesive fracture of an adhesive layer of Araldite® 2015 with thickness ( $t_A$ ) of 0.2 mm was simulated with a mixed-mode (I+II+III) CZM, whose detailed description can be found in the work of Campilho et al. [16]. A trapezoidal law between stresses and relative displacements between homologous points of the cohesive elements with zero thickness was considered, to account for the adhesive ductility [5, 11, 12]. The formulation allows a mixed-mode behaviour, in which damage onset is predicted using a quadratic stress criterion and failure with a linear energetic criterion. In the FE models, crack propagation with cohesive elements was only considered for the cohesive failure of

the adhesive bond. A stress-based criterion was assumed for the tensile failure of the composite parts. For the  $0^\circ$  plies, oriented with the load, the experimentally determined strength from unidirectional specimens was considered ( $1280 \pm 177$  MPa, the average value was used for the prediction of failure). For the  $90^\circ$  plies, i.e., experiencing a matrix failure, typical values from the literature were used ( $\approx 40$  MPa) [5]. In the numerical models, failure was predicted as the load of patch debonding onset [17], guaranteeing that neither the laminate nor the patch attained the mentioned strengths. The prospect of interlaminar and intralaminar failures near the scarf was not considered, despite the chance of this occurrence [5], owing to slightly smaller cohesive properties for these propagations compared with the properties of most structural adhesives. This procedure was adopted due to the modelling difficulties and additional computational time required to simulate these localized fractures, which do not influence by a significant amount the global characteristics of 3D repairs such as the ones proposed in this work. Under this simplification hypothesis, the predictions should be interpreted in relative terms between the different tested solutions, allowing the establishment of design principles for these repairs, instead of being viewed as precise quantitative predictions. The adhesive layer was introduced in the numerical models by the trapezoidal CZM, with experimentally defined properties for the specific value of  $t_A$  used in the repairs. The cohesive laws of the adhesive layer in pure-modes I and II were estimated in a previous work by the authors [5] by DCB (mode I) and ENF (mode II) tests with the same value of  $t_A$ , using an inverse technique. The pure mode III cohesive law was considered equal to the pure mode II one. A detailed description of the cohesive model, inverse determination of the cohesive parameters and respective discussion, and finally the properties of a  $t_A=0.2$  mm adhesive layer of Araldite® 2015 can be found in the aforementioned work by the authors [5].

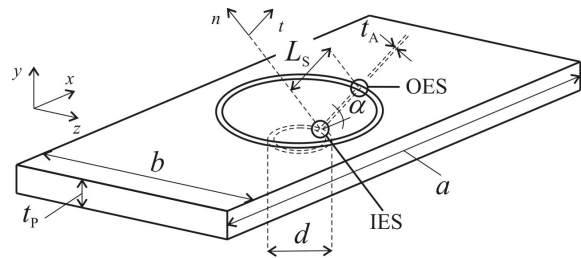


Figure 1. Scarf repair geometry.

Figure 1 shows the scarf repair geometry and characteristic dimensions. The Outer Edge of the Scarf (OES) and Inner Edge of the Scarf (IES) loci are also defined. The following dimensions were considered for the FE analysis:  $a=200$  mm,  $b=50$  and  $80$  mm,  $t_p=2.4$  mm,  $d=10$  mm,  $t_A=0.2$  mm and  $\alpha=10, 15, 25$  and  $45^\circ$  (for the repairs with  $b=50$  mm) or  $\alpha=5, 10, 15, 25$  and  $45^\circ$  (for the repairs with  $b=80$  mm). The minimum values of  $\alpha$  were imposed by the respective values of  $b$ . Sixteen plies and  $[0_2, 90_2, 0_2, 90_2]_S$  lay-up laminates and

patches were used in this analysis (0.15 mm ply unit thickness).

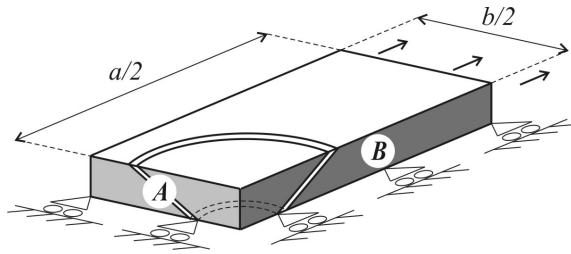


Figure 2. FE idealization with symmetry conditions.

Figure 2 represents the numerical idealization of the scarf repair tensile test. Only  $\frac{1}{4}$  of the laminate was modelled, by the use of symmetry conditions at the mid-transversal (A) and mid-longitudinal (B) planes. The scarf repairs were simulated in ABAQUS<sup>®</sup> with 3D models. The cohesive elements, used to simulate a cohesive failure of the adhesive layer, were introduced in the numerical models along the scarf. A geometrical non-linear analysis was performed, using 8-node hexahedral and 6-node pentahedral solid finite elements available in ABAQUS<sup>®</sup>. Figure 3 shows the mesh at the repaired region for the  $\alpha=15^\circ$  repair ( $b=50$  mm). The mesh is particularly refined at the scarf region, with forty elements along  $L_s$ , to ensure a bigger refinement at the loci of stress concentrations [7, 8].

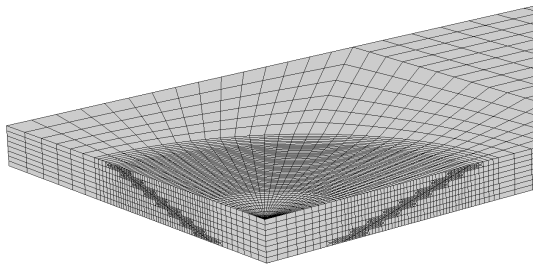


Figure 3. Detail of the mesh at the repaired region.

Thirty elements were considered for  $\frac{1}{4}$  of the patch in the radial direction. At the scarf region, each group of two equally oriented and adjacent plies was modelled with five solid elements. Mesh coarsening was applied to reduce the number of elements outside this region. The laminate and patch were modelled as elastic orthotropic, considering the properties of reference [18].

### 3. STRENGTH OF THE STANDARD SCARF REPAIRS

Figure 4 shows the load-displacement ( $P$ - $\delta$ ) curves for the different values of  $\alpha$ , considering  $b=50$  mm. The values of  $P$  and  $\delta$  are the direct output of the simulations, i.e., considering half-width and half-length of the repairs. The original curves were shifted ( $\Delta=0, 0.05, 0.10$  and  $0.15$  mm) for an easier visualization. An

identical stiffness of the repairs and increasing values of  $P$  were found with the decrease of  $\alpha$  [7, 8].

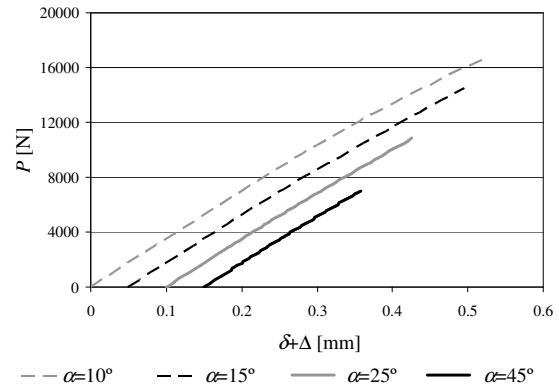


Figure 4. FE  $P$ - $\delta$  curves for different values of  $\alpha$ .

The stiffness reduction near the peak load is due to softening of the adhesive layer, in anticipation of patch debonding. Fracture of the repairs was identical for all the values of  $\alpha$ , with a simultaneous fracture of the adhesive at the entire bond near plane B after localized damage at the IES and OES, propagating swiftly in the radial direction of the scarf up to approximately  $45^\circ$  of plane B. An example of this fracture is presented in Fig. 5 for a  $\alpha=15^\circ$  repair ( $b=50$  mm).

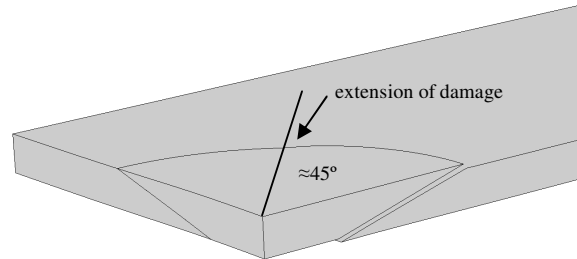


Figure 5. FE failure for a  $\alpha=15^\circ$  repair ( $b=50$  mm).

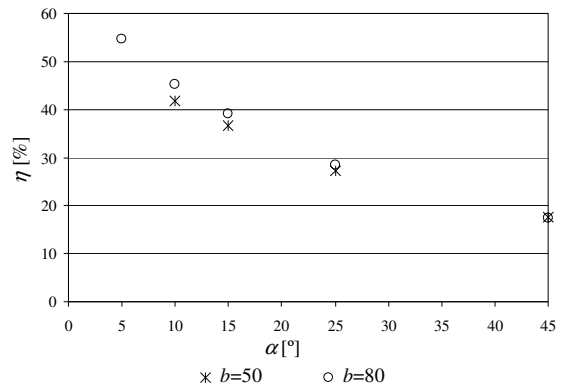


Figure 6.  $\eta$  as a function of  $\alpha$  for the repairs with  $b=50$  and  $80$  mm.

Figure 6 plots the efficiency of the repairs ( $\eta$ ) as a function of  $\alpha$  for the repairs with  $b=50$  and  $80$  mm.  $\eta$  is the quotient between the patch debonding onset load and the unnotched composite strength. The failure load was determined by tensile tests on three undamaged specimens with  $b=15$  mm and the same lay-up and thickness of the damaged laminates, giving an average value of failure stress and deviation of  $655\pm 134$  MPa. For the calculations of  $\eta$ , the average value was considered in the estimation of the failure load for the  $b=50$  and  $80$  mm undamaged laminates, using the respective cross-sectional areas. In all of the repairs, including in the study of Section 4, it was checked that the failure strength of the  $0^\circ$  and  $90^\circ$  plies was not attained prior to patch debonding onset. The exponential increase of  $\eta$  with the reduction of  $\alpha$  is related to the corresponding increase of the bond area [7, 8]. The values of  $\eta$  are slightly bigger for the repairs with  $b=80$  mm, with an increasing difference to the  $b=50$  mm repairs as  $\alpha$  diminishes, due to a larger influence of the laminate resistant area at the symmetry plane **A** on the global characteristics of the repairs for  $b=80$  mm, since the repair dimensions are similar for a given value of  $\alpha$ . The best results are always granted by the smallest value of  $\alpha$ , i.e.,  $\alpha=10^\circ$  for  $b=50$  mm ( $\eta\approx 42\%$ ) and  $\alpha=5^\circ$  for  $b=80$  mm ( $\eta\approx 55\%$ ).

#### 4. STRENGTH OF THE SCARF REPAIRS WITH OVER-LAMINATING PLYS

An alternative to the use of very small values of  $\alpha$ , required to fully restore the structure strength, consists on the application of external doublers (or over-laminating plies) adhesively-bonded at the repaired region to protect the patch tips and to provide a larger cross-sectional area at the repaired region, thus increasing the strength of the repairs [19]. These plies are generally very thin and designed to follow the parent structure contour as closely as possible. Although the most efficient solution is to bond over-laminating plies on both the laminate faces [20], a more practical solution consists on their application only on the outer face of the repair (upper surface in Fig. 1) [21]. This choice can also be imposed by accessibility difficulties to the inner face of the composite structure, or be rendered unfeasible for sandwich laminates with composite faces. In the present work, an optimization study was carried out on the influence of using over-laminating plies on the value of  $\eta$ , considering reinforcement only at the outer face of the repair (single reinforcement) and at both faces (double reinforcement). The over-laminate consisted of two plies of circular shape: a  $0^\circ$  ply adjacent to repair surface, covered by a  $90^\circ$  ply. Figure 7 shows the geometry for double reinforcement. Two overlaps with the damaged structure at the outer face ( $e$ ) were tested for the single reinforcement: 2.5 and 5 mm. For the double reinforcement, only  $e=5$  mm was considered. Bigger values were not considered, to guarantee a minimum

clearance with the repair edges for the smallest values of  $\alpha$  (for each value of  $b$ ).

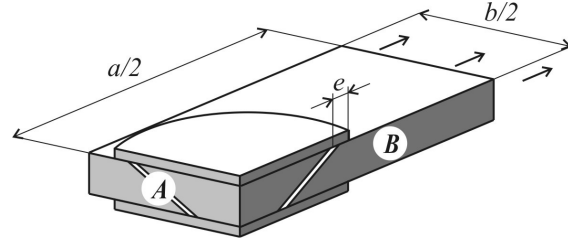


Figure 7. FE idealization of the scarf repair with double reinforcement.

Identical dimensions were considered for the reinforcements on both faces for fabrication simplification purposes and maximum effect of the over-laminates, although the inner face of the repairs may be over-reinforced [20]. Fracture for the different tested solutions depended on the type of reinforcement (single or double) and value of  $\alpha$ . For the single reinforcement and bigger values of  $\alpha$ , the asymmetry of loading induced by the over-laminating plies led to a slight transverse deflection of the laminate that caused premature crack initiation near plane **B** at the IES (unreinforced region). This damage then propagated towards the OES and to the overlap region, simultaneously to radial growth of damage towards plane **A**. Figure 8 (a) shows damage initiation at the IES for a  $\alpha=45^\circ$  repair with  $b=50$  mm and  $e=2.5$  mm.

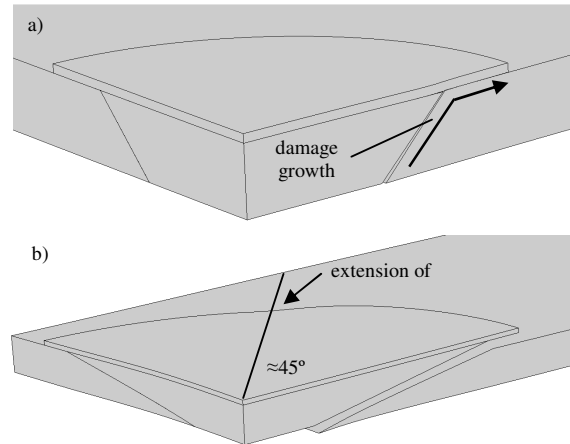


Figure 8. FE failure initiation for a  $\alpha=45^\circ$  repair (a) and failure for a  $\alpha=10^\circ$  repair (b) ( $e=2.5$  mm,  $b=50$  mm and reinforcement on the outer face).

For the smaller values of  $\alpha$ , fracture was simultaneous over the entire bond and overlap region. Although the transverse deflection of the repairs still subsisted, the bigger taper length in the laminate and patch allowed a slight bending of the scarf tips, enough to avoid a premature fracture at the IES. Figure 8 (b) relates to a  $\alpha=10^\circ$  repair with  $b=50$  mm and  $e=2.5$  mm.

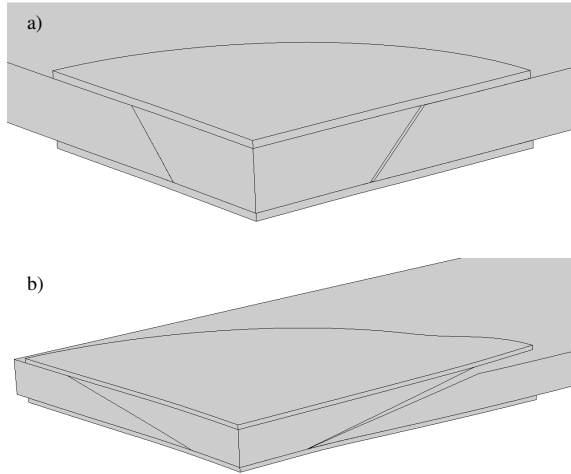


Figure 9. FE failure initiation for a  $\alpha=45^\circ$  repair (a) and failure for a  $\alpha=10^\circ$  repair (b) ( $e=2.5$  mm,  $b=50$  mm and double reinforcement).

The asymmetry of load induced by the over-laminating plies is prevented using double reinforcement. Thus, for the bigger values of  $\alpha$  the entire scarf bond failed simultaneously near plane **B**, whilst the overlapping plies were kept under load (Fig. 9 a). Increasing further the load causes the detachment of the over-laminate at the outer face, followed by the one at the inner face, both from plane **B** towards plane **A**. For the smaller values of  $\alpha$ , the overlap area between the reinforcement plies and the laminate is much larger for the inner plies than for the outer plies, which results on failure along the scarf bond and at the outer over-laminate, whilst the inner one is kept intact (Fig. 9 b). Figure 10 and Fig. 11 plot the values of  $\eta$  as a function of  $\alpha$  for the repairs with single and double reinforcement, respectively.

Figure 10 globally shows the exponential trends formerly mentioned, with an increasing difference in the value of  $\eta$  between the  $b=50$  and 80 mm repairs with the reduction of  $\alpha$ , whose cause was already discussed. The value of  $e$  showed a large impact on  $\eta$ , with bigger values being recommended on account of higher repair efficiency. This is due to the larger shear resistant area between the laminate and over-laminating plies. The highest efficiency for the  $b=50$  mm and 80 mm repairs (single reinforcement) was attained with the  $\alpha=10^\circ$  repair ( $\eta \approx 49\%$ ) and the  $\alpha=5^\circ$  repair ( $\eta \approx 62\%$ ), respectively. These results confirm a non-negligible improvement to the standard scarf repair (up to 20%). The results of Fig. 11 (double reinforcement) also evidence an increasing difference of  $\eta$  with the reduction of  $\alpha$  between the  $b=50$  and 80 mm repairs. The improvement of  $\eta$  was substantial, with the highest values for the  $b=50$  and 80 mm repairs being found for the  $\alpha=10^\circ$  repair ( $\eta \approx 58\%$ ) and the  $\alpha=5^\circ$  repair ( $\eta \approx 72\%$ ), respectively. These correspond to improvements to the unreinforced repair between 30 and 60%.

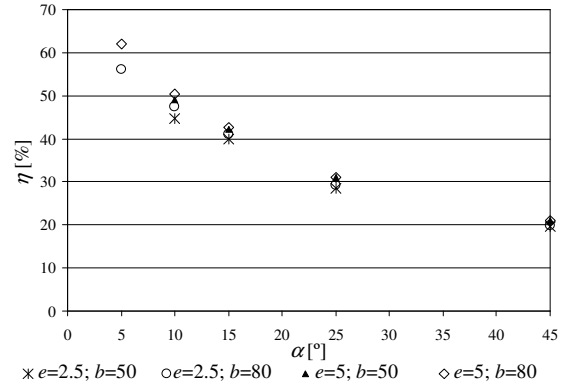


Figure 10.  $\eta$  as a function of  $\alpha$  for the repairs with single reinforcement (dimensions in mm).

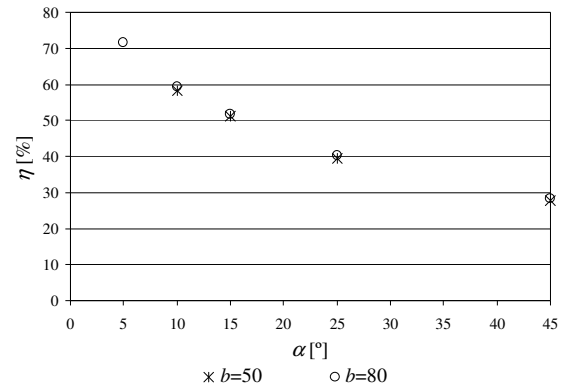


Figure 11.  $\eta$  as a function of  $\alpha$  for the repairs with double reinforcement (dimensions in mm).

## 5. CONCLUDING REMARKS

In this work, a numerical analysis was performed on the tensile behaviour of three-dimensional scarf repairs in carbon-epoxy structures, using a ductile adhesive (Araldite® 2015). The Finite Element analysis was performed in ABAQUS® and used Cohesive Zone Models for the simulation of damage onset and growth in the adhesive layer. Trapezoidal cohesive laws in each pure mode were used to account for the ductility of the adhesive. Validation of the Finite Element methodology used was performed in previous works, which assures the legitimacy of the results. A parametric study was performed on the scarf angle, considering two values of width for the laminates to be repaired. The strength improvement increased exponentially with the reduction of the scarf angle, which implies that small angles are always recommended. The use of over-laminating plies at the outer or both of the repair faces was tested as an attempt to increase the repairs efficiency, which for scarf repairs without over-laminate was close to 50% of the unnotched laminates strength, for the smallest scarf angle. Results showed that efficiencies of approximately

70% of the undamaged strength could be attained by the use of over-laminating plies on both the laminate faces, with maximum improvements from the scarf repairs without over-laminate between approximately 20 and 60%, depending on the scarf angle. Reinforcing only at the outer face of the repair, which may be the only feasible option due to accessing or disassembly difficulties, is also recommended, despite a smaller restitution of strength. Efficiencies above 70% could be achieved using smaller scarf angles than the ones tested, which would imply a larger width of the laminates to be repaired. This work allowed the establishment of principles to design scarf repairs. However, the presented quantitative predictions should be considered valid only for the specific set of conditions selected for the analysis, whilst the generic principles to increase the efficiency of scarf repairs are always recommended.

### REFERENCES

- [1] Chotard, T.J., Pasquier, J., Benzeggagh, M.L., "Residual performance of scarf-repaired pultruded shapes initially impact damaged", *Composite Structures*, vol. 53, pag. 317-331, 2001.
- [2] Smith, F.C., Moloney, L.D., Matthews, F.L., "Fabrication of woven carbon fibre/polycarbonate repair patches", *Composites Part A: Applied Science and Manufacturing*, vol. 27, pag. 1089-1095, 1996.
- [3] Soutis, C., Duan, D.M., Goutas, P., "Compressive behaviour of CFRP laminates repaired with adhesively bonded external patches", *Composite Structures*, vol. 45, pag. 289-301, 1999.
- [4] Sato, C., Ikegami, K., "Dynamic deformation of lap joints and scarf joints under impact loads", *International Journal of Adhesion & Adhesives*, vol. 20, pag. 17-25, 2000.
- [5] Campilho, R.D.S.G., de Moura, M.F.S.F., Pinto, A.M.G., Morais, J.J.L., Domingues, J.J.M.S., "Modelling the tensile fracture behaviour of CFRP scarf repairs", *Composites: Part B – Engineering*, vol. 40, pag. 149-157, 2009.
- [6] Bikerman, J.J., "The science of adhesive joints", New York, USA: Academic Press; 1968.
- [7] Wang, C.H., Gunnion, A.J., "On the design methodology of scarf repairs to composite laminates", *Composites Science and Technology*, vol. 68, pag. 35-46, 2008.
- [8] Campilho, R.D.S.G., de Moura, M.F.S.F., Domingues, J.J.M.S., "Stress and failure analyses of scarf repaired CFRP laminates using a cohesive damage model". *Journal of Adhesion Science and Technology*, vol. 21, pag. 855-970, 2007.
- [9] Kumar, S.B., Sridhar, I., Sivashanker, S., Osiyemi, S.O., Bag, A., "Tensile failure of adhesively bonded CFRP composite scarf joints", *Materials Science and Engineering: B*, vol. 132, pag. 113-120, 2006.
- [10] Odi, R.A., Friend, C.M., "A comparative study of finite element models for the bonded repair of composite structures", *Journal of Reinforced Plastics and Composites*, vol. 21, pag. 311-332, 2002.
- [11] Campilho, R.D.S.G., de Moura, M.F.S.F., Domingues, J.J.M.S., "Using a cohesive damage model to predict the tensile behaviour of CFRP single-strap repairs", *International Journal of Solids and Structures*, vol. 45, pag. 1497-1512, 2008.
- [12] Campilho, R.D.S.G., de Moura, M.F.S.F., Ramantani, D.A., Morais, J.J.L., Domingues, J.J.M.S., "Buckling behaviour of carbon-epoxy adhesively-bonded scarf repairs", *Journal of Adhesion Science and Technology*, vol. 23, pag. 1493-1513, 2009.
- [13] Pipes, R.B., Pagano, N.J., "Interlaminar stresses in composite laminates under uniform axial extension", *Journal of Composite Materials*, vol. 4, pag. 538-548, 1970.
- [14] Hart Smith, L.J., "Adhesive-bonded scarf and stepped-lap joints", Long Beach, USA: McDonnell-Douglas Corp.; 1973.
- [15] Qian, Z.Q., Akisanya, A.R., "An experimental investigation of failure initiation in bonded joints", *Acta Materialia*, vol. 46, pag. 4895-4904, 1998.
- [16] Campilho, R.D.S.G., de Moura, M.F.S.F., Ramantani, D.A., Morais, J.J.L., Domingues, J.J.M.S., "Tensile behaviour of three-dimensional carbon-epoxy adhesively-bonded single and double-strap repairs", *International Journal of Adhesion & Adhesives*, vol. 29, pag. 678-686, 2009.
- [17] Campilho, R.D.S.G., de Moura, M.F.S.F., Domingues, J.J.M.S., Morais, J.J.L., "Computational modelling of the residual strength of repaired composite laminates using a cohesive damage model", *Journal of Adhesion Science and Technology*, vol. 22, pag. 1565-1591, 2008.
- [18] Campilho, R.D.S.G., de Moura, M.F.S.F., Domingues, J.J.M.S., "Modelling single and double-lap repairs on composite materials", *Composites Science and Technology*, vol. 65, pag. 1948-1958, 2005.
- [19] Whittingham, B., Baker, A.A., Harman, A., Bitton, D., "Micrographic studies on adhesively bonded scarf repairs to thick composite aircraft structure", *Composites Part A: Applied Science and Manufacturing*, vol. 90, pag. 1419-1432, 2009.
- [20] Zimmerman, K., Liu, D., "Geometrical parameters in composite repair", *Journal of Composite Materials*, vol. 29, pag. 1473-1487, 1995.
- [21] Hamoush, S., Shivakumar, K., Darwish, F., Sharpe, M., Swindell, P., "Defective repairs of laminated solid composites", *Journal of Composite Materials*, vol. 39, pag. 2185-2196, 2005.